Cell Reports

Repeated Antigen Exposure Extends the Durability of Influenza-Specific Lung-Resident Memory CD8$^+$ T Cells and Heterosubtypic Immunity

Graphical Abstract

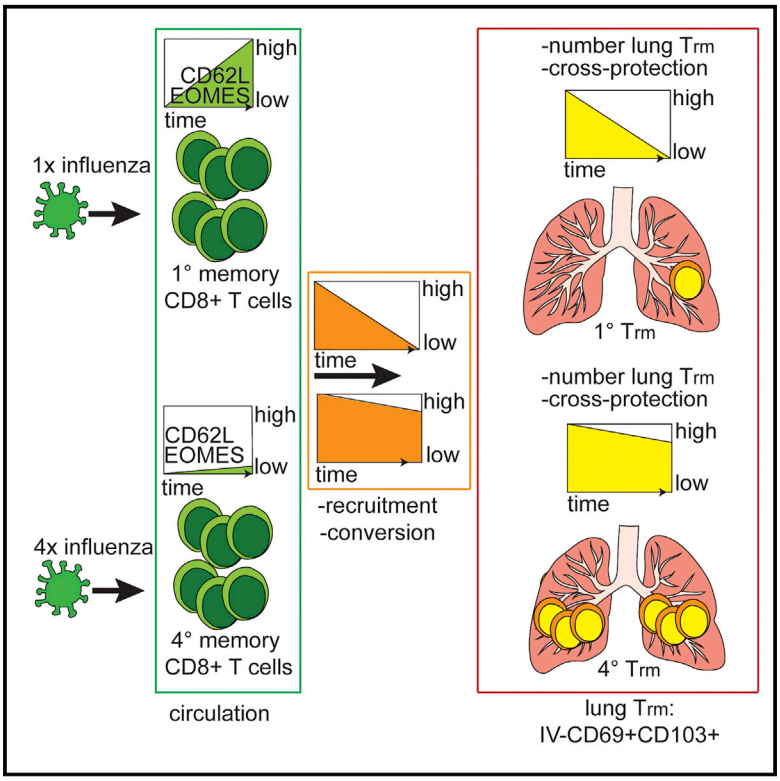

Highlights

- Influenza-specific quaternary (4°M) lung T_{rm} persist longer than 1°M T_{rm}
- Circulating 4°M CD8$^+$ T cells have prolonged T_{em} phenotype compared to 1°M CD8$^+$ T cells
- Circulating 4°M T_{em} exhibit sustained migration to the lung and conversion to T_{rm}
- Prolonged lung 4°M T_{rm} maintenance extends heterosubtypic immunity to influenza

Authors

Natalija Van Braeckel-Budimir, Steven M. Varga, Vladimir P. Badovinac, John T. Harty

Correspondence

john-harty@uiowa.edu

In Brief

Van Braeckel-Budimir et al. find that repeated antigen exposure by influenza virus infection in the lung enhances the durability of lung CD8$^+$ T resident memory populations and extends the duration of heterosubtypic immunity against influenza virus.

Van Braeckel-Budimir et al., 2018, Cell Reports *24*, 3374–3382
September 25, 2018
https://doi.org/10.1016/j.celrep.2018.08.073

CellPress

OPEN ACCESS
CellPress

Cell Reports
Report

Repeated Antigen Exposure Extends the Durability of Influenza-Specific Lung-Resident Memory CD8$^+$ T Cells and Heterosubtypic Immunity

Natalija Van Braeckel-Budimir,[1] Steven M. Varga,[1,2,3] Vladimir P. Badovinac,[1,2,3,4] and John T. Harty[1,2,3,4,5,*]
[1]Department of Microbiology and Immunology, University of Iowa, Iowa City, IA 52242, USA
[2]Department of Pathology, University of Iowa, Iowa City, IA 52242, USA
[3]Interdisciplinary Graduate Program in Immunology, University of Iowa, Iowa City, IA 52242, USA
[4]Senior author
[5]Lead Contact
*Correspondence: john-harty@uiowa.edu
https://doi.org/10.1016/j.celrep.2018.08.073

SUMMARY

Lung-resident primary memory CD8$^+$ T cell populations (T_{rm}) induced by a single influenza infection decline within months, rendering the host susceptible to new heterosubtypic influenza infections. Here, we demonstrate that, relative to single virus exposure, repeated antigen exposure dramatically alters the dynamics of influenza-specific lung T_{rm} populations. Lung T_{rm} derived from repeatedly stimulated circulating memory CD8$^+$ T cells exhibit extended durability and protective heterosubtypic immunity relative to primary lung T_{rm}. Parabiosis studies reveal that the enhanced durability of lung T_{rm} after multiple antigen encounters resulted from the generation of long-lasting circulating effector memory (T_{em}) populations, which maintained the ability to be recruited to the lung parenchyma and converted to T_{rm}, in combination with enhanced survival of these cells in the lung. Thus, generating a long-lasting T_{rm} precursor pool through repeated intranasal immunizations might be a promising strategy to establish long-lasting lung T_{rm}-mediated heterosubtypic immunity against influenza.

INTRODUCTION

Based on health and socioeconomic impact, influenza virus infections are a major global health burden (Kondrich and Rosenthal, 2017; Nicholson et al., 2003). This public health burden remains despite the approval of the first influenza vaccine almost 7 decades ago (Barberis et al., 2016). Current vaccine formulations aim for induction of neutralizing antibodies specific for the main surface antigen (hemagglutinin [HA]) of the influenza virus particle (Barberis et al., 2016). However, the HA protein undergoes high rates of mutation (antigenic drift) (Doherty et al., 2006) that enables successful escape from the immunological pressure of vaccination-induced antibodies and dramatically limits vaccine efficacy (Boni, 2008; de Jong et al., 2000). Additionally, reassortment of the segmented influenza virus genome in animal reservoirs can result in new HA sequences (antigenic shift) (Kim et al., 2018) that have not previously circulated in humans and have the potential for pandemic infections (Kim et al., 2018). It has been well documented in humans and rodent models that influenza-specific CD8$^+$ T cells targeting conserved internal proteins of the virus can control virus titers and limit disease development in the absence of neutralizing antibodies (Altenburg et al., 2015; Kreijtz et al., 2007; McMichael et al., 1983; Sridhar et al., 2013). Recent research suggests that the population of lung-resident CD8$^+$ T cells (T_{rm}) induced by primary influenza infection plays a critical role in such heterosubtypic immunity (HI) (Hogan et al., 2001; Slütter et al., 2017; Wu et al., 2014). Thus, inducing a potent and long-lasting influenza-specific T_{rm} population should be considered as a potentially useful vaccination target.

Waning of protection is one of the main limitations of T cell-mediated heterosubtypic immunity after primary influenza infection (Liang et al., 1994; Slütter et al., 2017; Wu et al., 2014). We and others have shown that the gradual loss of protection closely correlates with the decrease in size of the influenza-specific lung T_{rm} population (Slütter et al., 2017; Wu et al., 2014). Mechanistically, lung T_{rm} cells undergo increased apoptosis that, in combination with time-dependent decreases in recruitment and conversion of circulating T_{rm} precursors, limit the longevity of influenza-specific T_{rm} in the lung (Slütter et al., 2017). Of note, the vast majority of published studies addressing the formation and maintenance of influenza-specific lung T_{rm}, are based on a "single-exposure" model (Slütter et al., 2017; Takamura et al., 2016; Wu et al., 2014). This represents an important limitation given the repetitive, seasonal nature of influenza infections and the current approaches of yearly vaccine applications. Thus, it is pivotal to understand how repeated influenza antigen encounters impact the dynamics of lung T_{rm} and, consequently, the longevity of heterosubtypic immunity.

RESULTS

Experimental Model

To study the impact of repeated influenza infections on lung T_{rm}, we initially infected C57BL/6 mice with an antibody escape variant of the mouse adapted H1N1 A/PR/8, designated SEQ12 (Das et al., 2013; Van Braeckel-Budimir et al., 2017),

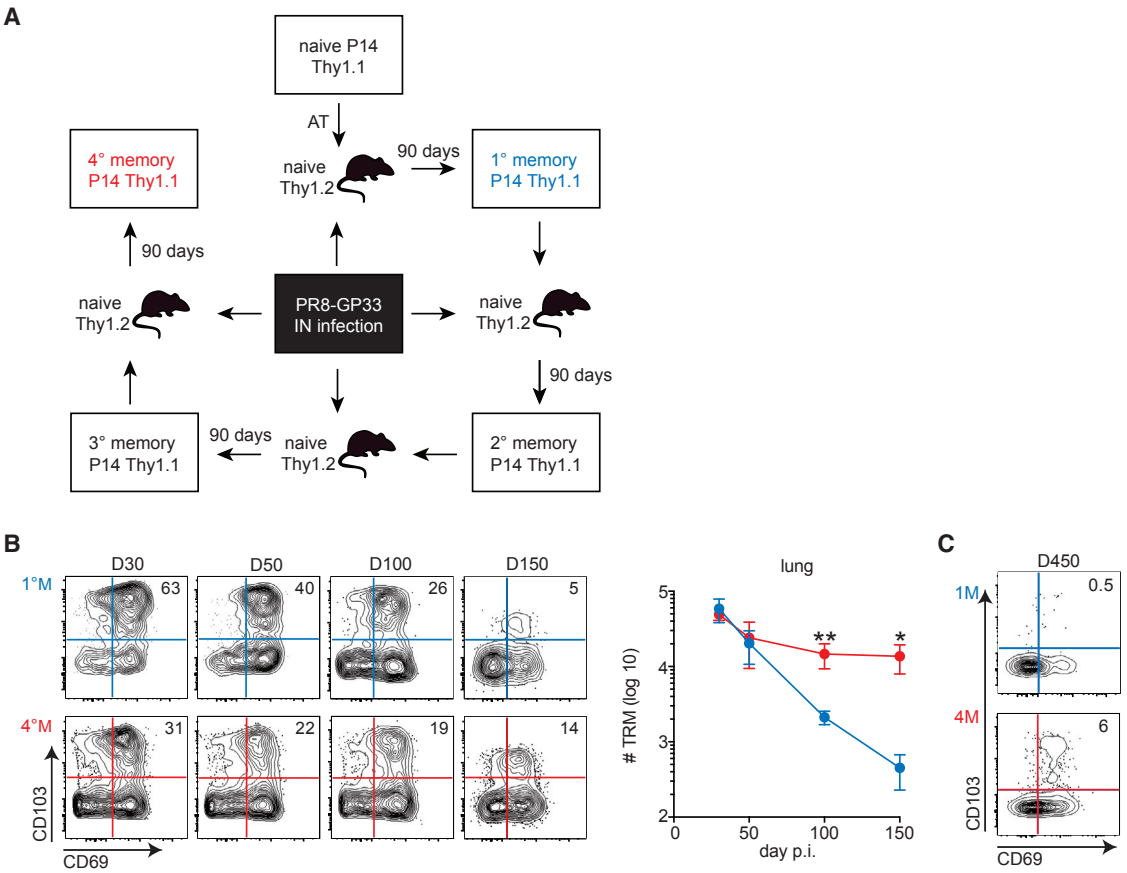

Figure 1. 4°M Lung T_{rm} Exhibits Increased Durability Relative to 1°M Lung T_{rm}

(A) Generation of memory $CD8^+$ T cells. A sequential P14 adoptive transfer approach and IN infection with PR8-GP33 were used to obtain 1°M (blue) and 4°M (red) T cell responses that could be analyzed simultaneously.

(B) Groups of mice bearing 1°M (blue) and 4°M (red) P14 cells were euthanized at days 30, 50, 100, and 150 p.i. Representative plots of % of CD69 and CD103 expression in IV^- P14 at the indicated time points (left). Cumulative results depicting numbers of T_{rm} ($IV^-CD69^+CD103^+$) in the lung (right). n = 3–4 mice/group. Representative of three independent experiments. Error bars represent mean ± SD. **p = 0.0034, *p = 0.0162, unpaired t test.

(C) Representative plot of lung IV^- P14 cells 450 days p.i. Percentages of $CD69^+CD103^+$ T_{rm} are indicated.

followed at 60-day intervals by infection with X31 (H3N2), and then a high dose of the parental A/PR/8 (PR8) virus. Despite the careful selection of viruses, sequential infection with SEQ12 and X31 induced antibodies that neutralized PR8 and no virus was recovered after the tertiary challenge (not shown). Furthermore, repeated infections may lead to generation of memory populations with different antigen exposure history, by incomplete recruitment of existing memory $CD8^+$ T cells together with *de novo* recruitment of naive $CD8^+$ T cells (Masopust et al., 2006; Wirth et al., 2010). Thus, we sought to develop a model that would allow us to generate distinct populations of T_{rm} with defined numbers of antigen encounters after lung infection.

To address these issues, we took advantage of a previously published model based on adoptive transfer (AT) of TCR transgenic $CD8^+$ T cells (Wirth et al., 2010). Naive Thy1.2 C57BL/6 mice were seeded with low numbers (10^4) of naive spleen-derived transgenic Thy1.1 P14 cells and subsequently intranasally (IN) infected with recombinant PR8 expressing the GP33 epitope of lymphocytic choriomeningitis virus (LCMV) recognized by P14 cells (PR8-GP33). Ninety days after infection, 10^5 spleen-derived primary memory (1°M) P14 $CD8^+$ T cells were transferred into new naive congenic recipients followed by IN infection with PR8-GP33. Simultaneously, another group of naive recipients was seeded with naive P14 cells and infected IN with PR8-GP33. Adoptive transfer and viral infections were repeated until we simultaneously obtained 1°M and quaternary memory (4°M) P14 cells (Figure 1A). Of note, based on published data indicating that 3°M cells proliferate less than naive CD8 T cells in response to systemic infection (Wirth et al., 2010) and in order to achieve similar frequencies of circulating 1°M and 4°M P14 cells, mice received 10^5 3°M P14 cells. This model not only permitted isolation and transfer of P14 cells with a known antigen exposure history but also incorporated the recently established notion that circulating memory T cells can be recruited to tissues and generate T_{rm} after repeated infections (Beura et al., 2018; Park et al., 2018). Figure S1A depicts selected phenotypic characteristics of naive and 3°M spleen-derived P14 which were the precursors of 1°M and 4°M lung

T_{rm}. Of note, the circulating precursor populations used for adoptive transfer lacked cells expressing both CD69 and CD103, which represent the canonical markers of lung T_{rm} (Wakim et al., 2013; Wu et al., 2014). As expected, naive and 3°M populations exhibited differential expression of a number of cell surface markers, including CD44, CD11a, CD62L, and KLRG1. To verify that the different numbers of transferred cells did not impact the overall course of influenza infection and to confirm that both 1°M and 4°M cells developed in similar conditions, we assessed the lung PR8-GP33 titers at different days after infection. As depicted in Figure S1B, titers measured 4 and 6 days after infection were similar in recipients of naive or 3°M P14 and in the same range as titers measured in mice receiving no adoptive transfer prior to infection. This finding suggested that the input of circulating naive or 3°M P14 did not alter the course of infection and that 1°M and 4°M cells developed under similar infection conditions. For clarity, although all of the recipient mice were infected with influenza only once, we will refer to mice bearing 1°M P14 cells as 1°M mice, and those bearing 4°M P14 cells as 4°M mice.

Multiple Antigen Encounters Enhance the Durability of Influenza-Specific Lung T_{rm}

To determine whether multiple antigen encounters altered the durability of lung T_{rm}, lungs of 1°M and 4°M mice were analyzed at different time points after the PR8-GP33 infection. To discriminate circulating cells from those within the tissue parenchyma, we performed intravascular (IV) exclusion based on IV injection of a fluorescently labeled pan-lymphocyte marker (CD45.2) 3 min prior to euthanasia as described (Galkina et al., 2005; Teijaro et al., 2011). T_{rm} were defined as $CD8^+IV^-CD69^+CD103^+$ based on our previous results (Slütter et al., 2017). As described earlier (Slütter et al., 2017; Wu et al., 2014), 1°M lung T_{rm} populations gradually waned over time, with only a few hundred cells detectable in the lung parenchyma 5 months after influenza exposure (Figure 1B). In sharp contrast, after an initial ~3-fold decline between day 30 and day 50 post-infection (p.i.), 4°M T_{rm} numbers stabilized and were maintained at >10,000 cells/lung out to day 150 p.i. As a result, the 4°M T_{rm} population was >50-fold larger than the 1°M T_{rm} population at day 150 after infection (Figure 1B). Strikingly, 4°M T_{rm} could be readily detected as late as day 450 p.i., a time point when 1°M T_{rm} have essentially disappeared (Figure 1C). Thus, multiple antigen encounters after lung infection extended the durability of influenza-specific lung T_{rm}.

Antigen Exposure History Defines the Tissue-Specific Distribution of Influenza-Specific $CD8^+$ T Cells without Altering the Basic T_{rm} Phenotype

Previous studies have emphasized the impact of repeated systemic infection on fundamental biological characteristics of memory $CD8^+$ T cells and their distribution in tissues (Jabbari and Harty, 2006; Masopust et al., 2006; Rai et al., 2014; Vezys et al., 2009; Wirth et al., 2010). Thus, we assessed whether and how the history of influenza antigen encounter impacted the distribution of memory $CD8^+$ T cells. To be able to study memory cell distribution while allowing for competition for distinct niches, we generated 1°M and 4°M cells in the same host (Figure S2A). For this purpose, naive Thy1.2/1.2 C57BL/6 recipients were seeded with mixture of 10^4 Thy1.1/1.2 naive P14 and 10^5 Thy1.1/1.1 3°M P14 cells and subsequently IN infected with PR8-GP33. Mice were analyzed at day 90 p.i., and the distribution of 1°M and 4°M cells was assessed in the spleen, blood, and lungs (Figure S2B). While the distribution of 1°M and 4°M cells was similar in the blood and spleen, 4°M cells were the dominant population in the lung, with slightly stronger preference for the parenchymal (IV^-) niche compared to the vasculature (IV^+) niche (Figure S2B).

Furthermore, we investigated whether repeated influenza antigen exposures altered some of the important phenotypic properties of lung T_{rm}. For this purpose, we evaluated expression of CD103, CD69 (classical T_{rm} markers) (Schenkel and Masopust, 2014; Wu et al., 2014), Eomes (a key transcription factor down-regulated in T_{rm}) (Mackay et al., 2015), CX3CR1 (expressed by T_{rm} precursors) (Gerlach et al., 2016), and CXCR3 (facilitates homing to the lung/airway) (Slütter et al., 2013) on 1°M and 4°M P14 generated in the same host (Figures S2A and S2C). Overall, we observed no substantial difference in selected phenotypic characteristics between 1°M and 4°M lung T_{rm}. Most 1°M and 4°M IV^-CD103^+ cells expressed CD69, had low expression of Eomes and CX3CR1, and were $CXCR3^+$. These data demonstrated that repeated influenza antigen exposure enhanced 4°M entry into the lung parenchyma, where some of the cells developed T_{rm} phenotypic characteristics similar to those of their 1°M T_{rm} counterparts. Thus, major changes in canonical T_{rm} properties did not appear to account for the persistence of 4°M T_{rm} in the lung parenchyma.

Repeated Influenza Antigen Exposures Extend the Half-Life of T_{rm} in the Lung by Increasing Cell Survival

As shown previously, 1°M T_{rm} have a relatively short half-life in the tissue parenchyma and exhibit higher frequencies of cells with active caspase 3/7 and decreased Bcl-2 expression compared to 1°M T_{rm} in skin (Slütter et al., 2017). In the light of these findings, we hypothesized that the 4°M T_{rm} population could exhibit prolonged survival in the lung relative to 1°M T_{rm}, leading to their longer persistence. To probe this notion, we labeled lung T_{rm} 90 days p.i. by IN inoculation of carboxyfluorescein diacetate succinimidyl ester (CFSE) (Legge and Braciale, 2003; Slütter et al., 2017). This approach labels all of the cells in the lung, with negligible labeling of cells in the other tissue compartments, and loss of CFSE signal with time relates to loss of labeled cells, not dilution due to proliferation (Slütter et al., 2017). To determine the initial level of labeling, we evaluated CFSE intensity in the lung T_{rm} at 1 hr post-inoculation (Figure 2A). At this time point, 100% of lung T_{rm} were $CFSE^+$ (Figure 2A). When mice were analyzed 120 hr after labeling, only ~20% of 1°M T_{rm} were $CFSE^+$, confirming the relatively short survival of this population in the lung. A significantly ($p = 0.0127$) larger fraction (>30%) of 4°M T_{rm} were $CFSE^+$ at the same time post-labeling (Figure 2A), suggesting prolonged survival of these cells in the lung. Additionally, 4°M T_{rm} exhibited higher expression of Bcl-2, relative to 1°M T_{rm} (Figure 2B), consistent with increased survival of this population in the tissue parenchyma. Finally, we observed a modest, but significant ($p < 0.05$) increase in the proportion of 1°M relative to 4°M T_{rm}

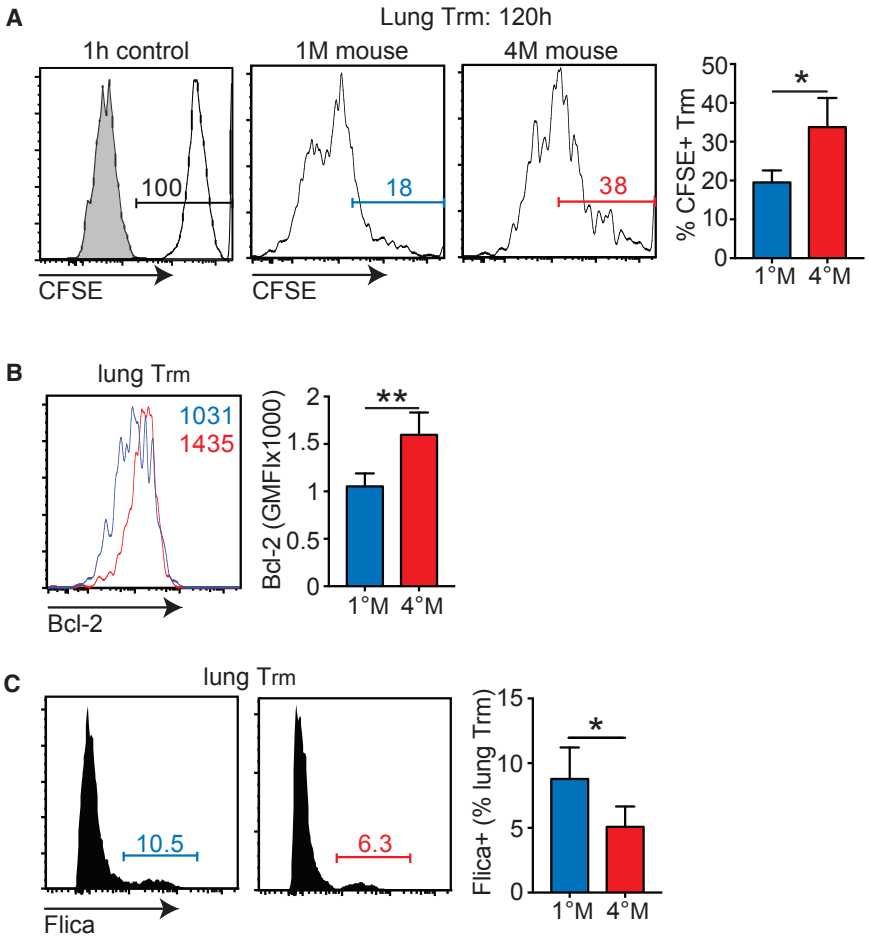

Figure 2. 4°M Lung T_{rm} Persists Longer and Exhibits Reduced Apoptosis Signature Compared to 1°M T_{rm}

(A) Mice bearing 1°M and 4°M P14 cells were IN inoculated with CFSE at day 90 p.i. and lung T_{rm} cells ($IV^{-}CD69^{+}CD103^{+}$) were analyzed 1 and 120 hr later. Representative flow plots of CFSE labeling (left) and cumulative analysis of percentage of CFSE-labeled cells 120 hr post-labeling (right). n = 4 mice/group. Representative of three independent experiments. Error bars represent mean ± SD. *p = 0.0127, unpaired t test.

(B) Bcl-2 expression by 1°M and 4°M lung T_{rm} measured 90 days p.i. Representative histograms (left); cumulative data (right). n = 4 mice/group. Representative of two independent experiments. Error bars represent mean ± SD. **p = 0.0072, unpaired t test. GMFI, geometric mean fluorescence intensity.

(C) Flica (caspase 3/7) staining of 1°M and 4°M lung T_{rm} measured 90 days p.i. Representative histograms (left); cumulative data (right). n = 4 mice/group. Representative of two independent experiments. Error bars represent mean ± SD. *p = 0.0435, unpaired t test.

cells staining positive with Flica reagent, suggesting increased proapoptotic caspase 3/7 activity (Figure 2C). Together, these results suggested that enhanced durability of 4°M T_{rm} in the lung parenchyma was due, at least in part, to increased survival. However, the differences in each "survival" assay were modest and are unlikely sufficient to entirely explain the enhanced durability of 4°M T_{rm}.

Repeated Influenza Antigen Exposures Stabilize the Circulating T_{rm} Precursor Pool

We previously showed that, despite their short half-life after CFSE labeling, 1°M T_{rm} are sustained for some time by recruitment to the lung of circulating effector memory (T_{em}) precursors, some of which undergo phenotypic and functional conversion to T_{rm} (Slütter et al., 2017). As a consequence of differentiation of circulating 1°M memory populations from T_{em} to primarily central memory (T_{cm}) with time, replenishment of lung T_{rm} eventually ceases and the population declines. Thus, we hypothesized that, due to their increased antigen exposure history, circulating 4°M may exhibit a sustained T_{em} population allowing for prolonged recruitment and conversion to lung T_{rm}. To probe this hypothesis, we took advantage of the mouse parabiosis model. 1°M mice, bearing Thy1.1/1.1 circulating memory and lung T_{rm} cells, and 4°M mice, bearing Thy1.1/1.2 circulating memory and lung T_{rm} cells, were surgically joined 90 days post-PR8-GP33 infection (Figure 3A). Three weeks later, parabiotic pairs were analyzed for the distribution of 1°M and 4°M P14 cells in blood, spleens, and lungs (Figure 3A). Of note, similar frequencies of circulating P14 were found in the blood and spleen of both groups (Figures 3B and 3C), indicating that equilibrium had been reached. However, this equilibrium did not reflect a 1:1 distribution of 1°M and 4°M circulating cells. Instead, both groups of mice exhibited 75% 1°M P14 and 25% 4°M P14 ratio in the blood and spleen (Figures 3B and 3C). In contrast, a higher frequency of memory P14 was recovered from the total lung and IV^{-} fraction of the lung in the 4°M parabiont (Figure 3D). As expected from prior work showing that late 1°M loses the ability to home to the lung parenchyma and convert to T_{rm} (Slütter et al., 2017), and despite the dominance of 1°M in the circulation, T_{rm} in the lungs of the 4°M parabiotic partner were exclusively 4°M T_{rm}. In contrast, despite their reduced presence in the circulation, a clear population of 4°M T_{rm} could be found within the T_{rm} population of the 1°M parabiotic partner (Figure 3D). These data suggested that circulating 4°M exhibited a prolonged capability to home to the lung parenchyma and convert to T_{rm}.

The contribution of 4°M T_{rm} P14 to the T_{rm} compartment in 1°M mice at 3 weeks of parabiosis was low (~5%). Thus, we investigated whether representation of these cells would increase with additional time of parabiosis. For this purpose, 1°M and 4°M parabiotic partners were euthanized 13 weeks after joining, and distribution of P14 cells in lung tissue was assessed.

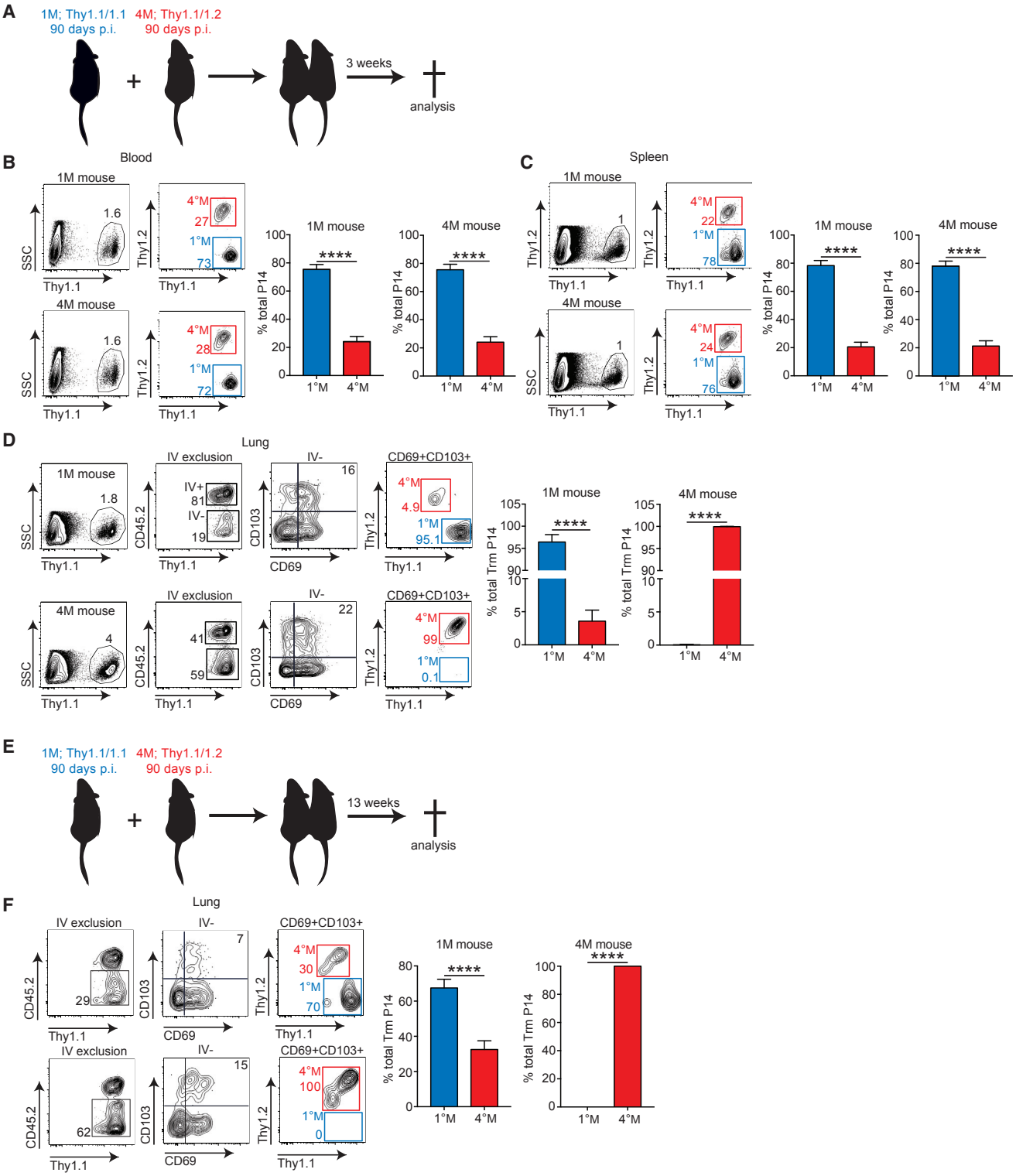

Figure 3. Circulating 4°M Cells Home to the Lung and Convert to T_{rm} for Extended Period of Time

(A) 90 days post-PR8-GP33 infection, mice bearing Thy1.1/1.1 1°M P14 (blue; "1°M mice") and Thy1.1/1.2 4°M P14 (red; "4°M mice") cells were joined by parabiosis. Three weeks later, parabionts were analyzed.

(B–D) Abundance of 1°M (blue) and 4°M (red) P14 cells in peripheral blood (B) and spleen (C) of parabiotic mice. Representative plots (left); cumulative data (right). n = 4 parabionts/experiment. Representative of two independent experiments. Error bars represent mean ± SD. ****$p < 0.0001$, unpaired t test.

(legend continued on next page)

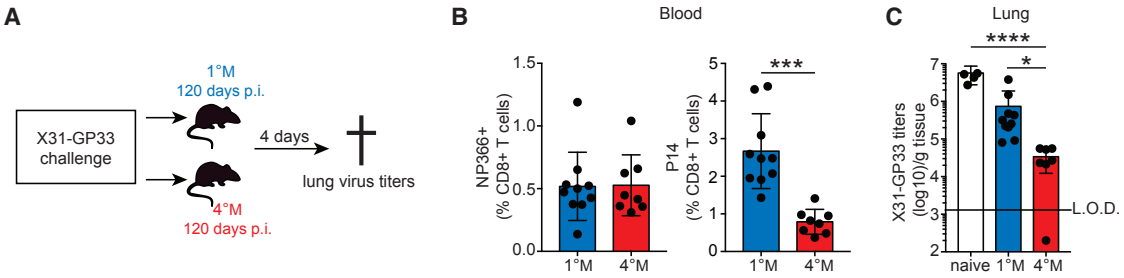

Figure 4. Durability of 4°M T_{rm} Cells Enable Long-Lasting Heterosubtypic Protection

(A) 120 days post-PR8-GP33 infection, mice bearing 1°M (blue) and 4°M (red) P14 cells were IN infected with 5 × 10^4 $TCID_{50}$ X31-GP33. 4 days after the challenge, mice were euthanized, and lung virus titers were assessed.

(B) Prior to challenge influenza NP366-specific (left) and P14 (right) $CD8^+$ T cell responses were evaluated in blood and expressed as percentage of total $CD8^+$ T cells in peripheral blood. n = 8–10 mice/group. Representative of two independent experiments. Error bars represent mean ± SD. ***p = 0.0001, unpaired t test.

(C) Lung X31-GP33 virus titers measured in naive mice, and mice bearing 1°M (blue) or 4°M (red) P14 cells. n = 5–10 mice/group. Representative of two independent experiments. Error bars represent mean ± SD. *p = 0.0216, ****p < 0.0001, Kruskal-Wallis test. L.O.D., limit of detection.

Extended time of parabiosis did not change the contributions of 1°M and 4°M cells to blood and spleen compartments of parabiotic partners (not shown). Despite the added time of parabiosis, we still detected no 1° T_{rm} in the lungs of the 4°M parabiotic partners. However, the representation of 4°M T_{rm} P14 increased from ~5% to ~30% in the lungs of the 1°M mice with the additional parabiosis time. These data suggested sustained accumulation of 4°M-derived T_{rm} from the circulating 4°M pool with time.

Consistent with this notion, splenic 1°M progressed from ~50% T_{em} ($CD62L^{lo}$) at day 50 p.i. to <10% T_{em} at day 150 p.i., and this resulted in a decrease in total numbers of splenic T_{em} (Figure S3A). In sharp contrast, the splenic 4°M population remained $CD62L^{lo}$ and the T_{em} population was numerically stable in the same time frame (Figure S3A). This trend was extended well beyond day 150, as even 7 months p.i. circulating 4°M continued to express a T_{em} phenotype ($CD62L^{lo}$) and a permissive transcription factor profile ($Eomes^{lo}$), whereas the 1°M population was exclusively T_{cm} ($CD62L^{hi}Eomes^{hi}$) at this late time point (Figure S3B). Although Tbet was modestly upregulated in 4°M, the Tbet regulated homing receptor CXCR3 was not differently expressed between splenic 1°M and 4°M (Figure S3C). These data were consistent with the notion that general impairment of lung-homing capacity was unlikely to underlie the failure to maintain 1°M T_{rm} (Slütter et al., 2017). In summary, circulating 4°M $CD8^+$ T cells, due to their prolonged display of T_{em} properties were recruited to the lung and converted into T_{rm} for an extended period of time, compared to circulating 1°M. Given the modest evidence for increased survival, sustained replenishment of lung T_{rm} from the circulatory memory pool likely accounted for the enhanced durability of 4°M lung T_{rm}.

Repeated Influenza Antigen Exposures Extend the Duration of the Heterosubtypic Protection

Waning of 1°M T_{rm} correlates strongly with loss of heterosubtypic immunity (Slütter et al., 2017; Wu et al., 2014). Our results show that multiple exposures of circulating $CD8^+$ T cell populations to pulmonary influenza infection extended the durability of lung T_{rm} far beyond that observed with 1°M lung T_{rm}. Thus, our next step was to investigate whether extending the durability of lung T_{rm} through multiple antigen exposures resulted in prolonged heterosubtypic immunity. For this purpose, 1°M mice and 4°M mice, from the cohorts analyzed in Figure 1C, were challenged with a high dose of the heterologous X31-GP33 virus 120 days post-PR8-GP33 exposure (Figure 4A). Heterosubtypic immunity was evaluated by measuring X31-GP33 titers in the lung of challenged mice (Figure 4A).

It is important to note that both groups of mice were exposed to PR8-GP33 only once, both contained similar percentages of endogenous 1°M $CD8^+$ T cells recognizing the NP366 influenza epitopes in their circulation, and challenge took place at a late time point when protection by endogenous lung T_{rm} would have waned (Figure 4B). Thus, potential differences in protection would be due to differences in lung P14 T_{rm} populations, which are lost in 1°M mice and sustained in 4°M mice (Figure 1C). While the magnitude of the endogenous influenza-specific 1°M responses were similar, in line with previous data (Figure 3) 1°M mice had higher circulating P14 frequencies than 4°M mice (Figure 4B) (Wirth et al., 2010). As expected at this late time point, 1°M memory mice showed only a modest reduction of X31-GP33 virus titers compared to naive infected mice, which did not reach statistical discernibility. In contrast, 4°M mice had ~99% less virus than the naive infected group (Figure 4C). Thus, the extended durability of

(D) Abundance and T_{rm} distribution of 1°M (blue) and 4°M (red) T_{rm} P14 cells expressed as a percentage of the total T_{rm} population ($IV^-CD69^+CD103^+$) in lungs of parabiotic mice. Representative plots (left); cumulative data (right).

(E) Parabionts were prepared as in (A) and were analyzed 13 weeks after the surgery.

(F) Abundance and T_{rm} distribution of 1°M (blue) and 4°M (red) T_{rm} P14 cells expressed as a percentage of the total T_{rm} population ($IV^-CD69^+CD103^+$) in lungs of parabiotic mice. Representative plots (left); cumulative data (right). n = 4 parabionts/experiment. Representative of two independent experiments. Error bars represent mean ± SD. ****p < 0.0001, unpaired t test.

4°M T_{rm} in the lung enabled superior heterosubtypic immunity at time points after infection when protection mediated by 1°M T_{rm} had waned.

DISCUSSION

Heterosubtypic immunity against influenza virus has been extensively studied in a single-infection mouse model of the disease (Budimir et al., 2012; Christensen et al., 2000; Furuya et al., 2010; Liang et al., 1994; Nguyen et al., 1999; Slütter et al., 2017; Wu et al., 2014). Recent studies show that heterosubtypic immunity mediated by 1°M $CD8^+$ T cells wanes over time, as a consequence of gradual loss of lung T_{rm} cells (Slütter et al., 2017; Wu et al., 2014). In the context of annual influenza outbreaks and the potential for yearly immunizations, it has remained unknown how multiple antigen exposures influence the formation and maintenance of lung T_{rm} and subsequent T_{rm}-mediated heterosubtypic protection. To address these important knowledge gaps, we modified a multiple antigen exposure strategy previously used to assess responses to systemic infections (Wirth et al., 2010), by stimulating circulating memory $CD8^+$ T cell populations with localized lung influenza infections. This approach allowed us to overcome limitations of repeated infections with influenza virus and to study homogeneous populations of memory $CD8^+$ T cells with well-defined influenza exposure history (Masopust et al., 2006; Wirth et al., 2010). Our results revealed that 4°M T_{rm} cells exhibit substantially increased durability in the tissue parenchyma compared to 1°M T_{rm}. Mechanistically, the enhanced durability of 4°M cells resulted from improved survival of this population in the lung and a dramatically extended capacity for the circulating 4°M cells to enter the lung parenchyma and convert to T_{rm}. These findings strongly suggest that, by inducing a long-lived T_{em} population, multiple influenza exposures license a circulating T_{rm} precursor pool for sustained seeding and conversion in the lung, thus extending the duration of heterosubtypic immunity.

Our prior studies in systemic infection models (Jabbari and Harty, 2006; Nolz and Harty, 2011) showed that the history of antigen exposures defines fundamental biological properties of circulating memory $CD8^+$ T cells, which jointly determine their main function—protection against subsequent infection. For example, 1°M and 2°M $CD8^+$ T cells show differential capacity to protect against acute and chronic infection, with 2°M cells establishing better control of acute LCMV Armstrong or *Listeria monocytogenes* infection, but failing to protect against chronic LCMV clone 13 infection (Jabbari and Harty, 2006; Nolz and Harty, 2011). Importantly, this difference in protective capacity was driven by differential tissue preferences of 1°M and 2°M $CD8^+$ T cells, determined by antigen exposure history. Furthermore, the previously described dramatic changes in gene expression signature between memory T cells with different antigen exposure histories, strongly suggests that a complex network of fundamental properties, defined by the number of antigen encounters, determines the protective capacity of memory $CD8^+$ T cells. Here, we show that, similar to systemic infections, repeated exposures of circulating memory $CD8^+$ T cells to influenza infection in the lungs determines their ability to persist as T_{rm} and provide heterosubtypic protection against lung infection. Although further work will be needed to address possible differences in the per-cell quality of protection between 1°M and 4°M lung T_{rm}, it is clear that 4°M T_{rm}, on a population level, provide superior protection, as they can successfully control virus replication even very late after initial infection, when protection mediated by 1°M cells is lost (Figure 4C).

We have previously shown that maintenance of lung 1°M T_{rm} is a dynamic process, defined by the short half-life and high apoptotic rate of these cells on one side and replenishment from circulating memory populations on the other (Slütter et al., 2017). Importantly, not all circulating memory populations exhibit the same capacity to home to the lung and convert to T_{rm} (Slütter et al., 2017). We have identified the population of circulating T_{em} cells ($CD62L^{lo}$) as precursors for lung T_{rm} cells, as their circulating T_{cm} counterparts were not able to successfully seed the tissue and convert to T_{rm}. As 1°M $CD8^+$ T cells differentiate toward a uniform T_{cm} phenotype with time (Martin et al., 2015), the number of potential T_{rm} precursors decreases, resulting in a gradual loss of 1°M lung T_{rm}. Of note, we previously showed that multiple encounters with systemic pathogens generate memory populations with sustained characteristics of T_{em} (Wirth et al., 2010). We now show that $CD8^+$ T cells that undergo multiple encounters with influenza-derived antigens after lung infections exhibit similarly sustained T_{em} characteristics (Figure S3G), allowing for extended recruitment of these cells to the influenza-experienced lung and their conversion to T_{rm} (Figures 3A–3F). Furthermore, we were able to find well-defined, albeit reduced populations of 4°M lung T_{rm} as late as 450 days after infection (Figure 1C), suggesting that their lung persistence, although dramatically extended, may still be limited. Given that circulating 4°M populations express exclusively a T_{em} phenotype as late as 210 days after influenza exposure, it is likely that a slow transition to T_{cm} is not the sole explanation for the eventual decline of 4°M lung T_{rm}. At this point, we cannot rule out that possible time-dependent changes in the architecture of the lung tissue and immunological landscape after influenza infection have an important impact on long-lasting maintenance of the lung T_{rm} population. These important knowledge gaps merit further in-depth studies in the realm of lung physiology in the context of influenza virus infection.

It is important to acknowledge that our study did not compare lung T_{rm} cells that encountered influenza once or multiple times due to repeated infection of the same host. Instead, we build on recent data describing the capacity of circulating memory $CD8^+$ T cells to be recruited to the site of infection and convert to T_{rm} (Beura et al., 2018; Park et al., 2018). Thus, we describe fundamental differences between T_{rm} populations that were established by recruitment from the pool of circulating $CD8^+$ T cells that were exposed to influenza lung infections once or multiple times, in an otherwise naive host. Understanding whether and how multiple influenza exposures shape the already existing lung T_{rm} population remains an important knowledge gap and a major challenge, given the limitations of the available animal models and potential ethical and sampling concerns with multiple experimental challenges of humans.

Current influenza vaccines are highly purified subunit or split-virion formulations (Soema et al., 2015; Wong and Webby,

2013), composed mainly of surface viral antigens (HA and neuraminidase [NA]), while conserved internal antigens (e.g., nucleoprotein [NP]) represent only a fraction of a split-virus vaccine (Soema et al., 2015). These vaccines aim at inducing neutralizing antibodies against surface antigens, such as HA. High mutation rate and antigenic plasticity of the main antibody targets can severely compromise the efficacy of seasonal influenza vaccines and preclude their efficacy against pandemic influenza (Boni, 2008; Kim et al., 2018). Thus, much effort is currently directed toward the concept of universal influenza vaccines. Although $CD8^+$ T cells targeting conserved viral epitopes cannot provide sterilizing immunity to influenza infection, cumulative evidence points toward induction of lung-residing memory $CD8^+$ T cells as a promising strategy to provide heterosubtypic immunity that could broadly limit influenza disease in humans (Kumar et al., 2017; Pizzolla et al., 2018). Our findings suggest that repeated lung immunizations with formulations containing conserved $CD8^+$ T cell target epitopes, might generate durable lung T_{rm} populations capable of sustained heterosubtypic immunity.

STAR★METHODS

Detailed methods are provided in the online version of this paper and include the following:

- KEY RESOURCES TABLE
- CONTACT FOR REAGENT AND RESOURCE SHARING
- EXPERIMENTAL MODEL AND SUBJECT DETAILS
  - Mice
- METHOD DETAILS
  - Adoptive Transfer of P14 and Memory Generation
  - Infection and Immunizations and Virus Titers
  - Tissue Preparation, T Cell Analysis, Flow Cytometry
  - Parabiotic Surgery
- QUANTIFICATION AND STATISTICAL ANALYSIS

SUPPLEMENTAL INFORMATION

Supplemental Information includes three figures and can be found with this article online at https://doi.org/10.1016/j.celrep.2018.08.073.

ACKNOWLEDGMENTS

We thank Lecia Epping and Lisa Hancox for technical assistance, Stacey Hartwig for virus preparations, and Scott Hensley (University of Pennsylvania) for the SEQ12 virus. This work was supported by NIH Grants AI42767 (to J.T.H.), GM113961 (to V.P.B.), AI114543 (to J.T.H. and V.P.B.), AI124093 (to S.M.V.), and T32AI007511 (to N.V.B.-B.).

AUTHOR CONTRIBUTIONS

N.V.B.-B., V.P.B., and J.T.H. designed experiments. N.V.B.-B. performed experiments and data analysis. S.M.V. provided crucial experimental reagents. N.V.B.-B., S.M.V., V.P.B., and J.T.H. contributed to writing and editing of the manuscript. N.V.B.-B. performed statistical analysis.

DECLARATION OF INTERESTS

The authors declare no competing interests.

Received: May 24, 2018
Revised: August 1, 2018
Accepted: August 24, 2018
Published: September 25, 2018

REFERENCES

Altenburg, A.F., Rimmelzwaan, G.F., and de Vries, R.D. (2015). Virus-specific T cells as correlate of (cross-)protective immunity against influenza. Vaccine *33*, 500–506.

Barberis, I., Myles, P., Ault, S.K., Bragazzi, N.L., and Martini, M. (2016). History and evolution of influenza control through vaccination: from the first monovalent vaccine to universal vaccines. J. Prev. Med. Hyg. *57*, E115–E120.

Beura, L.K., Mitchell, J.S., Thompson, E.A., Schenkel, J.M., Mohammed, J., Wijeyesinghe, S., Fonseca, R., Burbach, B.J., Hickman, H.D., Vezys, V., et al. (2018). Intravital mucosal imaging of $CD8^+$ resident memory T cells shows tissue-autonomous recall responses that amplify secondary memory. Nat. Immunol. *19*, 173–182.

Boni, M.F. (2008). Vaccination and antigenic drift in influenza. Vaccine *26* (*Suppl 3*), C8–C14.

Budimir, N., Huckriede, A., Meijerhof, T., Boon, L., Gostick, E., Price, D.A., Wilschut, J., and de Haan, A. (2012). Induction of heterosubtypic cross-protection against influenza by a whole inactivated virus vaccine: the role of viral membrane fusion activity. PLoS One *7*, e30898.

Christensen, J.P., Doherty, P.C., Branum, K.C., and Riberdy, J.M. (2000). Profound protection against respiratory challenge with a lethal H7N7 influenza A virus by increasing the magnitude of $CD8^+$ T-cell memory. J. Virol. *74*, 11690–11696.

Das, S.R., Hensley, S.E., Ince, W.L., Brooke, C.B., Subba, A., Delboy, M.G., Russ, G., Gibbs, J.S., Bennink, J.R., and Yewdell, J.W. (2013). Defining influenza A virus hemagglutinin antigenic drift by sequential monoclonal antibody selection. Cell Host Microbe *13*, 314–323.

de Jong, J.C., Beyer, W.E., Palache, A.M., Rimmelzwaan, G.F., and Osterhaus, A.D. (2000). Mismatch between the 1997/1998 influenza vaccine and the major epidemic A(H3N2) virus strain as the cause of an inadequate vaccine-induced antibody response to this strain in the elderly. J. Med. Virol. *61*, 94–99.

Doherty, P.C., Turner, S.J., Webby, R.G., and Thomas, P.G. (2006). Influenza and the challenge for immunology. Nat. Immunol. *7*, 449–455.

Furuya, Y., Chan, J., Regner, M., Lobigs, M., Koskinen, A., Kok, T., Manavis, J., Li, P., Müllbacher, A., and Alsharifi, M. (2010). Cytotoxic T cells are the predominant players providing cross-protective immunity induced by gamma-irradiated influenza A viruses. J. Virol. *84*, 4212–4221.

Galkina, E., Thatte, J., Dabak, V., Williams, M.B., Ley, K., and Braciale, T.J. (2005). Preferential migration of effector $CD8^+$ T cells into the interstitium of the normal lung. J. Clin. Invest. *115*, 3473–3483.

Gerlach, C., Moseman, E.A., Loughhead, S.M., Alvarez, D., Zwijnenburg, A.J., Waanders, L., Garg, R., de la Torre, J.C., and von Andrian, U.H. (2016). The chemokine receptor CX3CR1 defines three antigen-experienced CD8 T cell subsets with distinct roles in immune surveillance and homeostasis. Immunity *45*, 1270–1284.

Hogan, R.J., Usherwood, E.J., Zhong, W., Roberts, A.A., Dutton, R.W., Harmsen, A.G., and Woodland, D.L. (2001). Activated antigen-specific $CD8^+$ T cells persist in the lungs following recovery from respiratory virus infections. J. Immunol. *166*, 1813–1822.

Jabbari, A., and Harty, J.T. (2006). Secondary memory $CD8^+$ T cells are more protective but slower to acquire a central-memory phenotype. J. Exp. Med. *203*, 919–932.

Kim, H., Webster, R.G., and Webby, R.J. (2018). Influenza virus: dealing with a drifting and shifting pathogen. Viral Immunol. *31*, 174–183.

Kondrich, J., and Rosenthal, M. (2017). Influenza in children. Curr. Opin. Pediatr. *29*, 297–302.

Kreijtz, J.H., Bodewes, R., van Amerongen, G., Kuiken, T., Fouchier, R.A., Osterhaus, A.D., and Rimmelzwaan, G.F. (2007). Primary influenza A virus

infection induces cross-protective immunity against a lethal infection with a heterosubtypic virus strain in mice. Vaccine *25*, 612–620.

Kumar, B.V., Ma, W., Miron, M., Granot, T., Guyer, R.S., Carpenter, D.J., Senda, T., Sun, X., Ho, S.H., Lerner, H., et al. (2017). Human tissue-resident memory T cells are defined by core transcriptional and functional signatures in lymphoid and mucosal sites. Cell Rep. *20*, 2921–2934.

Legge, K.L., and Braciale, T.J. (2003). Accelerated migration of respiratory dendritic cells to the regional lymph nodes is limited to the early phase of pulmonary infection. Immunity *18*, 265–277.

Liang, S., Mozdzanowska, K., Palladino, G., and Gerhard, W. (1994). Heterosubtypic immunity to influenza type A virus in mice. Effector mechanisms and their longevity. J. Immunol. *152*, 1653–1661.

Mach, N., Gillessen, S., Wilson, S.B., Sheehan, C., Mihm, M., and Dranoff, G. (2000). Differences in dendritic cells stimulated *in vivo* by tumors engineered to secrete granulocyte-macrophage colony-stimulating factor or Flt3-ligand. Cancer Res. *60*, 3239–3246.

Mackay, L.K., Wynne-Jones, E., Freestone, D., Pellicci, D.G., Mielke, L.A., Newman, D.M., Braun, A., Masson, F., Kallies, A., Belz, G.T., and Carbone, F.R. (2015). T-box transcription factors combine with the cytokines TGF-β and IL-15 to control tissue-resident memory T cell fate. Immunity *43*, 1101–1111.

Martin, M.D., Kim, M.T., Shan, Q., Sompallae, R., Xue, H.H., Harty, J.T., and Badovinac, V.P. (2015). Phenotypic and functional alterations in circulating memory CD8 T cells with time after primary infection. PLoS Pathog. *11*, e1005219.

Masopust, D., Ha, S.J., Vezys, V., and Ahmed, R. (2006). Stimulation history dictates memory CD8 T cell phenotype: implications for prime-boost vaccination. J. Immunol. *177*, 831–839.

McMichael, A.J., Gotch, F.M., Noble, G.R., and Beare, P.A. (1983). Cytotoxic T-cell immunity to influenza. N. Engl. J. Med. *309*, 13–17.

Mueller, S.N., Langley, W.A., Li, G., García-Sastre, A., Webby, R.J., and Ahmed, R. (2010). Qualitatively different memory $CD8^+$ T cells are generated after lymphocytic choriomeningitis virus and influenza virus infections. J. Immunol. *185*, 2182–2190.

Nguyen, H.H., Moldoveanu, Z., Novak, M.J., van Ginkel, F.W., Ban, E., Kiyono, H., McGhee, J.R., and Mestecky, J. (1999). Heterosubtypic immunity to lethal influenza A virus infection is associated with virus-specific $CD8^+$ cytotoxic T lymphocyte responses induced in mucosa-associated tissues. Virology *254*, 50–60.

Nicholson, K.G., Wood, J.M., and Zambon, M. (2003). Influenza. Lancet *362*, 1733–1745.

Nolz, J.C., and Harty, J.T. (2011). Protective capacity of memory $CD8^+$ T cells is dictated by antigen exposure history and nature of the infection. Immunity *34*, 781–793.

Park, S.L., Zaid, A., Hor, J.L., Christo, S.N., Prier, J.E., Davies, B., Alexandre, Y.O., Gregory, J.L., Russell, T.A., Gebhardt, T., et al. (2018). Local proliferation maintains a stable pool of tissue-resident memory T cells after antiviral recall responses. Nat. Immunol. *19*, 183–191.

Pizzolla, A., Nguyen, T.H., Sant, S., Jaffar, J., Loudovaris, T., Mannering, S.I., Thomas, P.G., Westall, G.P., Kedzierska, K., and Wakim, L.M. (2018). Influenza-specific lung-resident memory T cells are proliferative and polyfunctional and maintain diverse TCR profiles. J. Clin. Invest. *128*, 721–733.

Rai, D., Martin, M.D., and Badovinac, V.P. (2014). The longevity of memory CD8 T cell responses after repetitive antigen stimulations. J. Immunol. *192*, 5652–5659.

Schenkel, J.M., and Masopust, D. (2014). Tissue-resident memory T cells. Immunity *41*, 886–897.

Slütter, B., Pewe, L.L., Kaech, S.M., and Harty, J.T. (2013). Lung airway-surveilling $CXCR3^{hi}$ memory $CD8^+$ T cells are critical for protection against influenza A virus. Immunity *39*, 939–948.

Slütter, B., Van Braeckel-Budimir, N., Abboud, G., Varga, S.M., Salek-Ardakani, S., and Harty, J.T. (2017). Dynamics of influenza-induced lung-resident memory T cells underlie waning heterosubtypic immunity. Sci. Immunol. *2*, eaag2031.

Soema, P.C., Kompier, R., Amorij, J.P., and Kersten, G.F. (2015). Current and next generation influenza vaccines: formulation and production strategies. Eur. J. Pharm. Biopharm. *94*, 251–263.

Sridhar, S., Begom, S., Bermingham, A., Hoschler, K., Adamson, W., Carman, W., Bean, T., Barclay, W., Deeks, J.J., and Lalvani, A. (2013). Cellular immune correlates of protection against symptomatic pandemic influenza. Nat. Med. *19*, 1305–1312.

Takamura, S., Yagi, H., Hakata, Y., Motozono, C., McMaster, S.R., Masumoto, T., Fujisawa, M., Chikaishi, T., Komeda, J., Itoh, J., et al. (2016). Specific niches for lung-resident memory $CD8^+$ T cells at the site of tissue regeneration enable CD69-independent maintenance. J. Exp. Med. *213*, 3057–3073.

Teijaro, J.R., Turner, D., Pham, Q., Wherry, E.J., Lefrançois, L., and Farber, D.L. (2011). Cutting edge: tissue-retentive lung memory CD4 T cells mediate optimal protection to respiratory virus infection. J. Immunol. *187*, 5510–5514.

Van Braeckel-Budimir, N., Martin, M.D., Hartwig, S.M., Legge, K.L., Badovinac, V.P., and Harty, J.T. (2017). Antigen exposure history defines CD8 T cell dynamics and protection during localized pulmonary infections. Front. Immunol. *8*, 40.

Vezys, V., Yates, A., Casey, K.A., Lanier, G., Ahmed, R., Antia, R., and Masopust, D. (2009). Memory CD8 T-cell compartment grows in size with immunological experience. Nature *457*, 196–199.

Wakim, L.M., Gupta, N., Mintern, J.D., and Villadangos, J.A. (2013). Enhanced survival of lung tissue-resident memory $CD8^+$ T cells during infection with influenza virus due to selective expression of IFITM3. Nat. Immunol. *14*, 238–245.

Wirth, T.C., Xue, H.H., Rai, D., Sabel, J.T., Bair, T., Harty, J.T., and Badovinac, V.P. (2010). Repetitive antigen stimulation induces stepwise transcriptome diversification but preserves a core signature of memory $CD8^+$ T cell differentiation. Immunity *33*, 128–140.

Wong, S.S., and Webby, R.J. (2013). Traditional and new influenza vaccines. Clin. Microbiol. Rev. *26*, 476–492.

Wu, T., Hu, Y., Lee, Y.T., Bouchard, K.R., Benechet, A., Khanna, K., and Cauley, L.S. (2014). Lung-resident memory CD8 T cells (TRM) are indispensable for optimal cross-protection against pulmonary virus infection. J. Leukoc. Biol. *95*, 215–224.

STAR★METHODS

KEY RESOURCES TABLE

REAGENT or RESOURCE	SOURCE	IDENTIFIER
Antibodies		
Anti-mouse CD8α (clone 53-6.7)	BioLegend	Cat# 100725
Anti-mouse CD90.2 (clone 30-H12)	BuiLegend	Cat# 105306
Anti-mouse CD90.1 (clone OX-7)	BioLegend	Cat# 202504
Anti-mouse CD45.2 (clone 104)	BioLegend	Cat# 109832
Anti-mouse CD103 (clone 2E7)	BioLegend	Cat# 121406
Anti-mouse CD69 (cloneH1.2F3)	BioLegend	Cat# 104512
Anti-mouse CD44 (clone IM7)	eBioscience	Cat# 11-0441-82
Anti-mouse CD11a (clone M17/4)	eBioscience	Cat# 11-0111-85
Anti-mouse CD62L(clone MEL-14)	eBioscience	Cat# 17-0621-83
Anti-mouse Vβ8.1/8.2 (clone KJ16-133)	eBiosciences	Cat# 11-5813-82
Anti-mouse Vα2 (clone B20.1)	eBiosciences	Cat# 47-5812-80
Anti-mouse KLRG1 (clone 2F1)	eBioscience	Cat# 12-5893-82
Anti-mouse CXCR3 (clone CXCR3-173)	eBioscience	Cat# 11-1831-82
Anti-mouse CX3CR1 (clone SA011F11)	BioLegend	Cat# 149016
Anti-mouse Bcl2 (clone BCL/10C4)	BioLegend	Cat# 633508
Anti-mouse Eomes(clone Dam11Mag)	eBioscience	Cat# 12-4875-82
Anti-mouse Tbet(clone 4B10)	BioLegend	Cat# 644810
Tetramers		
H-2D^{b}-NP$_{366-374}$	*Prepared In house*	NA
Other reagents used for flow cytometry		
LIVE/DEAD® Fixable Aqua	Thermo Fisher Scientific	Cat# L34957
Brilliant Violet BV421 Streptavidin	BioLegend	Cat# 405225
Vybrant FAM Caspase-3 and −7 Assay Kit	Thermo Fisher Scientific	Cat# V35118
Chemical and Peptides		
5(6)-Carboxyfluorescein diacetate N-succinimidyl ester	Sigma-Aldrich	21888-25MG-F
Collagenase Type II	GIBCO	17101-015
DNase	Sigma-Aldrich	D4513-1VL
Percoll	GE Healthcare	Cat# 17-0891-01
VitaLyse	CMDG	Cat# WBL0100
Commercial Assays		
Anti-PE MicroBeads	Miltenyi Biotec	Cat# 130-048-801
Experimental models: Cell lines		
Mouse: primary lymphocytes	This manuscript	NA
Flt-3L tumor cell line	(Mach et al., 2000)	B16-FLT3L (RRID:CVCL_IJ12)
Experimental models: Organisms/Strains		
Mouse: C57BL/6J	National Cancer Institute	#556
Mouse: LCMV P14 TCR Tg	Harty lab	NA
Recombinant influenza PR8-GP33 virus	(Mueller et al., 2010)	NA
Recombinant influenza X31-GP33 virus	(Mueller et al., 2010)	NA
Software and Algorithms		
Diva 8	BD Biosciences	http://www.bdbiosciences.com
FlowJo v10	FlowJo, LLC	http://www.flowjo.com/solutions/flowjo/

CONTACT FOR REAGENT AND RESOURCE SHARING

Further information and requests for resources and reagents should be directed to and will be fulfilled by the Lead Contact, John T. Harty (john-harty@uiowa.edu).

EXPERIMENTAL MODEL AND SUBJECT DETAILS

Mice

Thy1.2/Thy1.2 C57BL/6 mice were purchased from the National Cancer Institute (Fredericksburg, MD). Thy1.1/Thy1.1 P14 TCR transgenic mice (on a C57BL/6 background) were originally acquired from Michael Bevan (University of Washington) and were maintained by brother sister mating in house. Thy1.1/Thy1.2 P14 TCR-tg mice were generated by crossing Thy1.1/Thy1.1 P14 TCR transgenic mice with Thy1.2 C57BL/6 mice in house. Mice used in all the experiments were female 6-10 weeks of age. All animal studies and procedures were approved by the University of Iowa Animal Care and Use Committee, under U.S. Public Health Service assurance, Office of Laboratory Animal Welfare guidelines.

METHOD DETAILS

Adoptive Transfer of P14 and Memory Generation

For generation of 1°M $CD8^+$ T cell response, peripheral blood cells from naive P14 TCR-transgenic mice were isolated, washed and characterized by flow cytometry for the frequency of $Vb8.1,8.2^+$ $Va2^+$ P14 TCR-tg T cells. Cell populations containing 10^4 naive Thy1.1. P14 cells were transferred iv in a 200 ul volume of sterile saline into naive C57BL/6 (Thy1.2) recipients. To transfer memory P14 cells, influenza PR8-GP33 immune mice were euthanized 90 days post infection, spleens were disrupted mechanically, made into a single cell suspension and stained with anti-Thy1.1-PE (clone Ox-7, Biolegend, San Diego, CA) in PBS with 5% FCS and subsequently purified using magnetic anti-PE beads (Mylteni, San Diego, CA) (Wirth et al., 2010). Purity of the population after enrichment was assessed by flow cytometry and ranged from 70%–85%. A cell mixture containing 10^5 memory Thy1.1 P14 cells was injected into naive Thy1.2 C57BL/6 mice. 2°M, 3°M and 4°M memory P14 responses were initiated by IN infection of recipient mice with PR8-GP33 24h after the adoptive transfer.

Infection and Immunizations and Virus Titers

Mice were immunized by IN infection with a sublethal dose of recombinant influenza PR8-GP33 virus ($2x10^4$ $TCID_{50}$) (Mueller et al., 2010), and protection was assessed by measuring lung virus titers defined as tissue culture infective dose 50 (TCID50) using MDCK cells after high-dose ($8x10^4$ $TCID_{50}$) X31-GP33 (Mueller et al., 2010) IN challenge. Both viruses were grown on chicken eggs. Virus-containing allantoic fluid was diluted in phosphate-buffered saline (PBS), and mice were inoculated with the specific viral dose after induction of anesthesia by ketamine + xylazine (80-100 mg/kg + 10-12.5 mg/kg) injection.

Tissue Preparation, T Cell Analysis, Flow Cytometry

For quantification of antigen-specific memory $CD8^+$ T cells, influenza immune mice were euthanized at the indicated time points p.i., 3 min after IV administration of 2 μg fluorescently labeled anti-CD45.2 antibody (IV exclusion) (Slütter et al., 2017). Spleen and PBL were harvested and processed into a single-cell suspension. Lungs were cut into small pieces and incubated in the presence of collagenase (125 U/ml) and deoxyribonuclease (0.1 mg/ml) for 1h at 37°C. After incubation a single-cell suspension was obtained by physical homogenization through a 70-μm cell strainer. Leukocytes were enriched by centrifugation in 35% Percoll (GE Healthcare) diluted in HBSS and red blood cells were lysed using Vitalize (BioE). For flow cytometry analyses, single cell suspensions were incubated 30 min at 4°C with the indicated antibodies and then washed extensively prior to analysis. Samples were stained for Thy1.1 to identify P14 cells or in house prepared MHC class I tetramers for D^b-$NP_{366-374}$ and analyzed by flow cytometry to identify transgenic P14 cells or endogenous influenza specific T cells and expression of the indicated markers detected with anti-CD8 (clone 53-6.7, eBioscience), anti-Thy1.2 (clone 30-H12, eBioscience), anti-Thy1.1 (clone OX-7, eBioscience), anti-CD45.2 (clone 104, BioLegend), anti-CD103 (clone 2E7, BioLegend), anti-CD69 (clone H1.2F3, BioLegend), anti-CD44 (clone 1M7, BioLegend), anti-CD11a (clone M17/4, eBioscience), anti-CD62L (clone MEL-14, BioLegend), anti-KLRG1 (clone 2F1, eBioscience), anti-CX3CR1 (clone SA011F11), anti-CXCR3 (clone CXCR3-173, eBioscience), anti-CX3CR1 (clone SA011F11, BioLegend), anti-Eomes (clone Dan11mag, eBioscience), Anti-mouse Bcl2 (clone BCL/10C4, eBioscience), Anti-mouse Tbet (clone 4B10 eBioscience). Active caspase3/7 (Flicka) staining was performed using Vybrant FAM Caspase-3 and −7 assay kit (Thermo Fischer Scientific, Waltham, MA) according to the manufacturer's protocol. Lung residing cells were labeled by IN administration of 70 ug of 5(6)-Carboxyfluorescein diacetate N-succinimidyl ester (CFSE) in 100 ul of PBS. Flow cytometry data were acquired using LSRFortessa (Becton Dickinson) and analyzed using the FlowJo software (FlowJo, LLC.).

Parabiotic Surgery

Mice bearing 1°M (Thy1.1/1.1) and 4°M (Thy1.1/1.2) P14 cells were surgically conjoined 90 days after PR8-GP33 infection. Parabionts were cohoused for two weeks prior to surgery. Two days prior to surgery skin preparation was performed. Under ketamine

anesthesia hair was removed from one side of the first mouse by shaving, starting approximately 1 cm above the elbow to 1 cm below the knee. Hair was then removed from the opposite side of the second mouse.

On the day of the surgery mice were anesthetized using ketamine/xylazine and injected subcutaneously with Meloxicam to induce analgesia. Once anesthesia was induced, mice were transferred to the surgery area, and the shaved skin was aseptically cleaned with betadine and alcohol. Mice were placed back to back, on their sides, with adjacent shaved areas facing up. To avoid contamination of the surgical area, mice were covered with a sterile surgical drape exposing only the surgical area. To prevent hypothermia, mice were positioned on the heat pad for the duration of the surgery.

Longitudinal skin incisions were performed on the shaved side of each animal, starting at ~0.5cm above the elbow to ~0.5cm below the knee joint. Skin was gently detached from the subcutaneous tissue and the separation was performed along the entire incision. After attachment of knee and elbow joints with non-absorbable 3-0 suture the skin of the two animals was connected with a continuous absorbable 5-0 suture starting ventrally from the elbow toward the knee. Once ventral skin attachment was completed with a double surgical knot, the suture was continued dorsally ending with a double surgical knot. Bupivacaine was applied locally to both sutures and each mouse was subcutaneously injected with sterile saline to prevent dehydrataion.

To prevent bacterial infections, animals were fed an antibiotic-containing diet starting from day 2 prior to surgery until day 10 post surgery. Mouse recovery was followed daily for two weeks after the procedure.

QUANTIFICATION AND STATISTICAL ANALYSIS

Statistical differences between two study groups were evaluated using an unpaired, two-tailed t test. Statistical differences between more than two study groups (single factor) were evaluated using one-way ANOVA with Tukey's multiple comparison post hoc test. Two-way ANOVA with Sidak's multiple comparison post hoc test was used to assess comparison between more than two groups based on more than one parameter (multiple factors). Statistical significance was assigned as $*p < 0.05$, $**p < 0.01$, $***p < 0.001$ and $****p < 0.0001$. Statistical analyses were performed using Prism 7 software (GraphPad).

Cell Reports, Volume *24*

Supplemental Information

Repeated Antigen Exposure Extends the Durability of Influenza-Specific Lung-Resident Memory $CD8^+$ T Cells and Heterosubtypic Immunity

Natalija Van Braeckel-Budimir, Steven M. Varga, Vladimir P. Badovinac, and John T. Harty

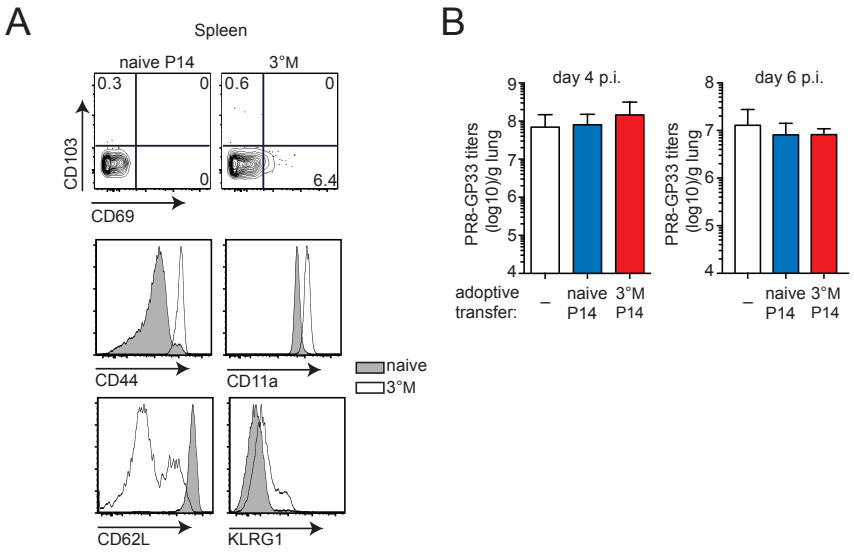

Figure S1: Characterization of adoptively transferred cells and their impact on PR8-GP33 infection. Related to figure 1.

(A) Phenotypic characterization of spleen-derived naive and 3°M P14 used for adoptive transfer and generation of 1°M and 4°M responses. (B) Naive C57Bl/6 recipients were seeded with 10^4 naive or 10^5 3°M P14 cells. 24h later these mice and naive mice were IN infected with PR8-GP33. PR8-GP33 virus titers measured at d4 and d6 p.i. in lungs of mice that received no P14 transfer (white), naive P14 transfer (blue) or 3°M P14 transfer (red). *n*=3-5 mice/group. Representative of 2 independent experiments. Error bars represents mean±SD. No significant differences, Kruskal-Wallis test.

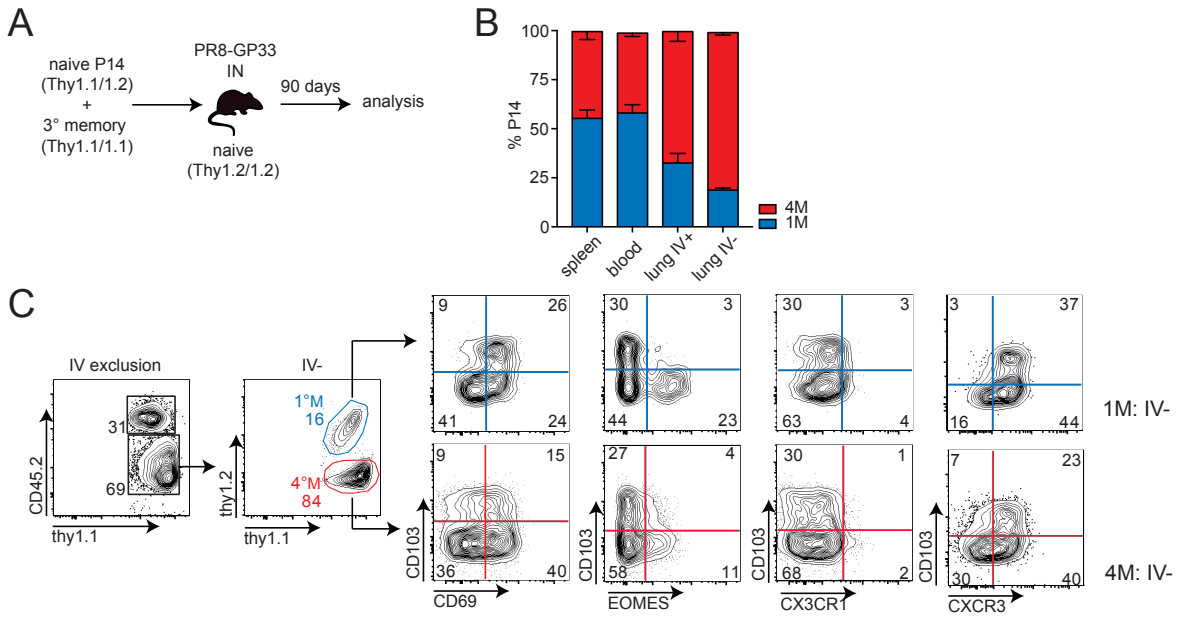

Figure S2: Tissue distribution and phenotypic characterization of 1°M and 4°M P14 cells. Related to figure 1. (A) Naive Thy1.2/1.2 C57Bl/6 mice were seeded with a mixture of 10^4 naive Thy1.1/1.2 and 10^5 3°M P14 cells. 24h later mice were IN infected with PR8-GP33. Mice were analyzed 90 days p.i. (B) Distribution of 1°M and 4°M P14 cells in various tissue compartments expressed as a % of total P14. *n*=3 mice/group. Representative of 2 independent experiments. Error bars represent mean±SD. Two-way ANOVA with Tukey's multiple comparison test. Statistic summary: 1°M – blue (spleen vs bld ns; spleen vs lung IV^+ **p=0.0011; spleen vs lung IV^- ****p<0.0001; blood vs lung IV^+ ***p=0.003; blood vs lung IV^- ****p<0.0001; lung IV^+ vs lung IV^- ns); 4°M – red (spleen vs blood ns; spleen vs lung IV^+ **p=0.0011; spleen vs lung IV^- ****p<0.0001; blood vs lung IV^+ ***p=0.0002; blood vs lung IV^- ****p<0.0001; lung IV^+ vs lung IV^- ns). (C) Representative plots of phenotypic characterization of lung residing IV^- 1°M (blue) and 4°M (red) P14 cells.

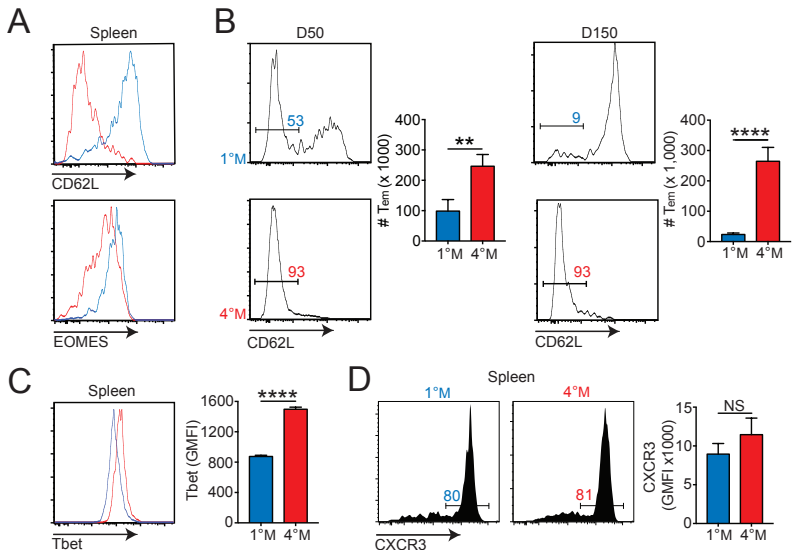

Figure S3: Changes in T_{em}-defining and lung-homing properties of circulating 1°M and 4°M P14 cells. Related to figure 3.

(A) Expression of CD62L by spleen-derived 1°M (blue) and 4°M (red) P14 cells (representative histograms, left) and numbers of $CD62L^{lo}$ T_{em} cells (cumulative bar graphs, right) at D50 and D150 p.i. *n*=4 mice/group. Representative of 2 independent experiments. Error bars represent mean±SD. **p=0.0016, ****p<0.0001, unpaired t test. (B) Representative histograms of expression of CD62L and EOMES by spleen-derived 1°M (blue) and 4°M (red) P14 cells 7 months p.i. (C) Expression of Tbet and (D) CXCR3 by spleen-derived 1°M (blue) and 4°M (red) P14 cells at D150 p.i. Representative histograms (left); cumulative data (right). *n*=4 mice/group. Representative of 2 independent experiments. Error bars represent mean±SD. ****p<0.0001, unpaired t test.